Substrate-supported carbon nanoscroll oscillator

Yuan Cheng [a], Xinghua Shi [b], Nicola M. Pugno [c,*], Huajian Gao [b,*]

[a] Institute of High Performance Computing, Singapore 138632, Singapore
[b] Division of Engineering, Brown University, 610 Barus and Holley, 182 Hope Street, Providence, RI 02912, USA
[c] Laboratory of Bio-Inspired Nanomechanics "Giuseppe Maria Pugno", Department of Structural Engineering, Politecnico di Torino, Corso Duca degli Abruzzi 24, 10129, Torino Italy

ARTICLE INFO

ABSTRACT

A substrate-supported carbon nanoscroll (CNS) oscillator is demonstrated through molecular dynamics simulations. By tuning the effective surface energy of CNS to a certain range (e.g., via an applied electric field), a substrate-supported CNS whose core is constrained by an inserted carbon nanotube can be made to oscillate around an equilibrium configuration at frequencies on the order of 10 GHz. It is found that stiffer core insertions lead to smaller damping coefficient and higher oscillating frequency, while temperature has a pronounced influence on the oscillating amplitude.

© 2011 Elsevier B.V. All rights reserved.

1. Introduction

Carbon nanoscrolls (CNS), corresponding to a graphene sheet rolled up into a scroll-shaped structure [1–4], have been of increasing interest due to their unique structural [5–9], dynamical [6], and electronic properties [4,10]. In contrast to carbon nanotubes (CNTs), the core size of the CNSs can be tuned by changing system parameters such as the effective surface energy via an applied electric field [11,12].

Oscillators constructed from nanomaterials, such as double-walled carbon nanotubes (DWCNTs) [13] or oscillation of C_{60} inside a single-walled carbon nanotube (SWCNT) [14], have been extensively studied. Most of these oscillators were CNT-based, with oscillatory motions along the axis of the tubes. An exception is the recently proposed CNS-based breathing oscillator [15]. In the present study, we demonstrate a type of substrate-supported CNS oscillator through molecular dynamics (MD) simulations. Compared to previously studied oscillators, the substrate-supported CNS oscillator moves in the direction perpendicular to the axis of the CNS. Once the core size of the CNS is constrained (e.g., by inserting a CNT), the dynamic motion of a CNS on substrate could be controlled by tuning the effective surface energy via an applied DC/AC electric field [16]. Here we show that, within a certain range of the effective surface energy, such a CNS can also be made to oscillate around an equilibrium configuration. The oscillation is driven by a potential energy well dominated by the van der Waals (VDW) interaction. The rigidity and size of the core insertion have a great influence on the oscillatory behavior of CNS on substrate, while temperature affects

the oscillating magnitude. Comparison with the motion of a multi-walled carbon nanotube (MWCNT) on substrate shows that the motion of CNS-based oscillator can be guided and controllable, which may offer unique advantages over MWCNT-based oscillators on substrate.

2. Methods

The model system of a CNS-based oscillator on substrate was constructed from two layers of graphene sheets with the dimension of 53.9×3.7 nm^2. The bottom layer served as the substrate while the upper one was rolled up into a CNS, as shown in Fig. 1A. DWCNT was inserted into the CNS, both as a template for rolling up of the CNS and as a way to constrain its core size to facilitate linear motion [16]. The DWCNT was composed with two SWCNTs with type (5, 5) and (10, 10).

The bonded interaction among all the carbon atoms was described by a Morse bond, a harmonic cosine of the bending angle, and a twofold torsion potential. The Lennard–Jones potential was used to describe the non-bonded interactions $U(r_{ij},\lambda) = 4\lambda\varepsilon[(\sigma/r_{ij})^{12}-(\sigma/r_{ij})^{6}]$, where $\varepsilon = 0.3601$ kJ/mol, $\sigma = 0.34$ nm, and λ is a tuning parameter used to control the interactions between different components of the system. For example, λ_{CC} denotes the CNS–CNS interaction parameter, and λ_{CS} denotes the CNS–substrate interaction. Here we keep the CNS–substrate interaction unchanged by fixing $\lambda_{CS} = 0.8$, while λ_{CC} is the tuning parameter mimicking the effect of an applying electric field on the CNS [12].

All simulations were performed using software Gromacs4 [17]. During MD simulations, the right end (Fig. 1) of the CNS was fixed on the rigid substrate. NVE ensemble with periodic boundary condition was used. An initial temperature of 10 K was adopted.
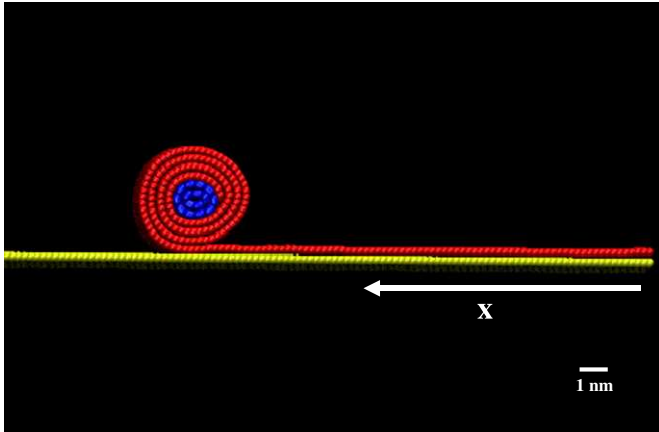
Fig. 1. A partially folded equilibrium configuration of a CNS on a graphene substrate. A DWCNT has been inserted to constrain the core of the CNS.

3. Results and discussion

3.1. Oscillation of CNS on substrates

As shown in our earlier work [16], if we define x as the length of the rolled out part of the CNS on substrate, the energy change associated with linear motion can be described as (driving force f)

$$f = -\frac{\delta V}{\delta x} = -\frac{\delta \Gamma_{CS} - \delta \Gamma_{CC}}{\delta x} - \frac{\delta W}{\delta x} \tag{1}$$

where V is the potential energy of the system, Γ_{CC} is the CNS–CNS interaction energy, Γ_{CS} is the CNS–substrate interaction energy, and W is the elastic bending energy. The motion of the CNS on substrate is controlled by the competition between the folding and unfolding driving forces, with VDW energy playing the dominant role. Γ_{CC} and Γ_{CS} are linearly correlated to λ_{CC} and λ_{CS}, respectively. As shown in Fig. 1, if a sufficiently large value of λ_{CC} is adopted, the interlayer interaction dominates and the nanoscroll folds up and moves rightward, while if a small value of λ_{CC} is selected, the CNS eventually unfolds and moves leftward. Within a certain range of intermediate values of λ_{CC}, a partially folded equilibrium configuration of CNS can be found, and the CNS can be made to oscillate around this equilibrium. In MD simulations, λ_{CC} was systematically varied for a range of partially folded equilibrium configurations of CNS and the oscillatory behavior of the CNS around these equilibrium positions was then studied. For example, the oscillatory behavior of the configuration shown in Fig. 1 was observed when $0.91 < \lambda_{CC} < 0.94$. The trajectory of the center of mass (COM) of the CNS as a function of the simulation time at $\lambda_{CC} = 0.94$ is shown in Fig. 2. The CNS oscillates at a frequency of $\omega \sim 8.5$ GHz with damping coefficient $\varsigma = 0.016$. Here ς is calculated as $\varsigma = 1/\sqrt{1 + (2\pi/\delta)^2}$, where $\delta = (1/n)\ln(x_0/x_n)$ is the logarithmic decrement, x_0 and x_n being two amplitude peaks separated by n periods.

The total potential energy of the system dissipates during the simulation time, and its variations are consistent with the position of the CNS, as shown in Fig. 3. The energy dissipation has no apparent correlation with the frequency of oscillation. The sum of CNS–CNS and CNS–substrate VDW energy is illustrated in Fig. 4, which indicates a potential well at the equilibrium position, and the oscillatory motion is dominantly driven by the VDW energy. While it is not intuitive that such an energy well would exist in a seemingly translationally invariant motion, we believe that the observed potential minimum can be attributed to an energy barrier associated with the edge of the graphene sheet wrapped inside the elastically deformed core of the CNS, as shown in Fig. 1.
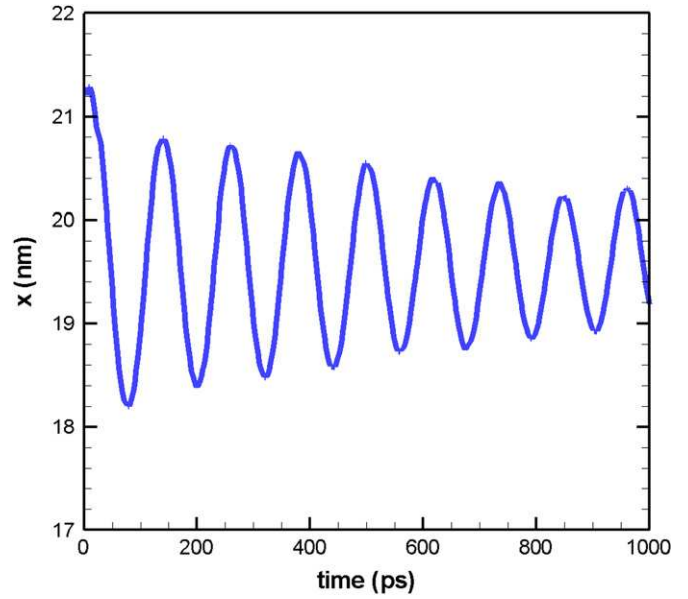

Fig. 2. The position of the CNS in the x-direction as a function of the simulation time.
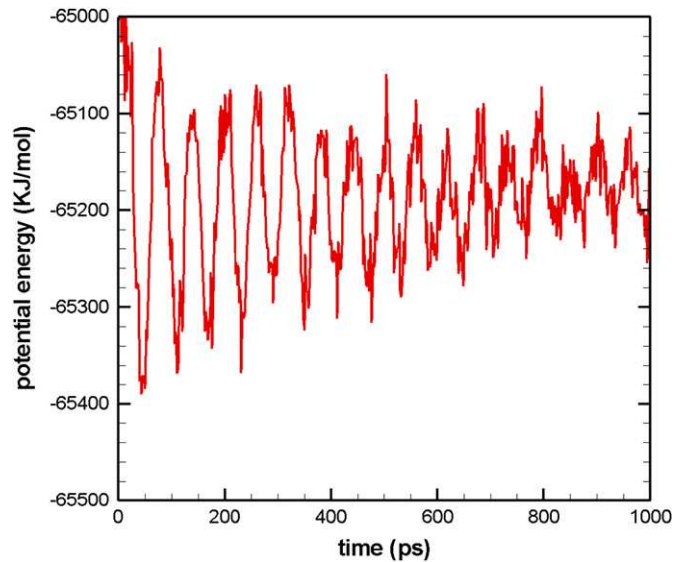

Fig. 3. Potential energy of the CNS as a function of the simulation time.

We note that the substrate-supported CNS linear oscillator works only within a certain range of λ_{CC} (e.g., $0.91 < \lambda_{CC} < 0.94$ for the configuration shown in Fig. 1). Within the working range, the frequencies of the oscillator are roughly the same. For the same CNS–substrate system, the working range of λ_{CC} also depends on the equilibrium configuration of the CNS. Suppose the positive direction is defined as going leftward, and x_1, x_2 denote the positions of the CNS in two different equilibrium configurations. When $x_2 > x_1$, a relative value of $\lambda_{CC2} < \lambda_{CC1}$ is observed at equilibrium. For example, for a less folded CNS located at $x = 29.45$ nm, the equilibrium occurs at $\lambda_{CC} = 0.83$. This is different from our earlier work on CNS-based breathing oscillator [15], where a wide range of λ_{CC} was adopted to induce oscillation. By tuning λ_{CC} (e.g., via an electric field), we can not only control the folding and unfolding motion of the CNS on substrate [16], but also design the oscillation of the CNS at a targeted location on the substrate.
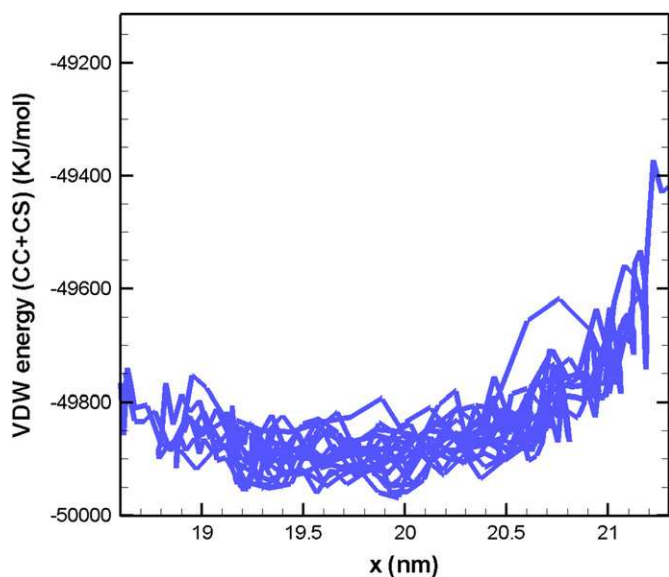
Fig. 4. Sum of the VDW interaction energy between CNS–CNS and CNS–graphene as a function of the position of the CNS.

Fig. 5. The position of the CNS in the *x*-direction as a function of the simulation time for two values of the flexibility parameter ϕ.

Fig. 6. Snapshot of CNS at 200 ps using a flexibility factor of $\phi = 1$.

3.2. Effect of rigidity of insertion on oscillatory behavior

Several factors can affect the oscillatory behavior of the CNS-based oscillator. Besides the strength of CNS–CNS and CNS–substrate interactions, the mechanical property of the core insertion can also influence the oscillatory behavior of the CNS.

In an earlier work proposed by Andreev et al. [18], the flexibility of CNTs was controlled by multiplying the angular, torsional, and non-bonded terms of the carbon–carbon interaction potential by a factor of $10^{-\phi}$, where ϕ is the flexibility parameter. Here we follow a similar strategy for defining the flexibility of the insertion. The simulation was repeated several times with varied values of ϕ. For example, $\phi = -1$ implies a very rigid core insertion. We take $\lambda_{CC} = 0.94$ while keeping other control parameters of the MD simulations unchanged. The COM position of the CNS on substrate is shown in Fig. 5. With a more rigid insertion, the oscillator has a higher frequency. The damping coefficient is $\varsigma = 0.006$, much smaller than the case with $\phi = 0$.

Further MD simulations were carried out taking $\phi = 1$. In this case the DWCNT insertion is more flexible and the snapshot of the MD simulation at 200 ps is shown in Fig. 6. If the insertion is too soft, we found that the CNS core can no longer be constrained and the motion becomes uncontrolled. This observation again confirms our earlier observation that a rigid insertion is necessary to induce controllable linear motion of a CNS on substrate [16], see also Ref. [19].

3.3. Effect of insertion size on oscillatory behavior of CNS

It has been shown that the core of the CNS must be constrained in order to achieve controllable oscillation of CNS on substrate [16]. In addition, the size of the insertion can also be designed to control the oscillatory behavior of CNS. To demonstrate this effect, for the same dimension of CNS and substrate, a MWCNT composed of three SWCNTs of types (5, 5), (10, 10), (15, 15) was inserted into the CNS. The oscillatory behavior was studied and the initial configuration was taken as the CNS at the position of $x = 12.1$ nm. The oscillatory behavior occurred at $\lambda_{CC} = 0.89$, and the trajectory is shown in Fig. 7.

Compared to the oscillator with a DWCNT insertion, the frequency of the oscillator with a larger insertion is lower, and the oscillatory period is longer. This can be explained by the
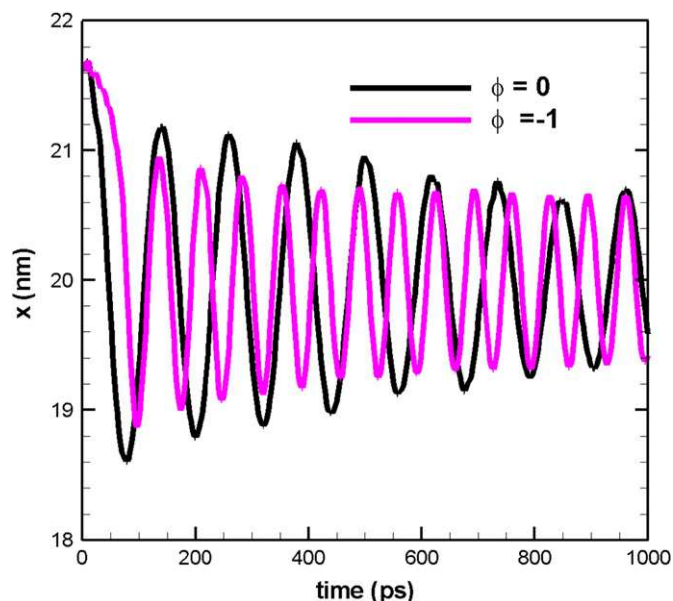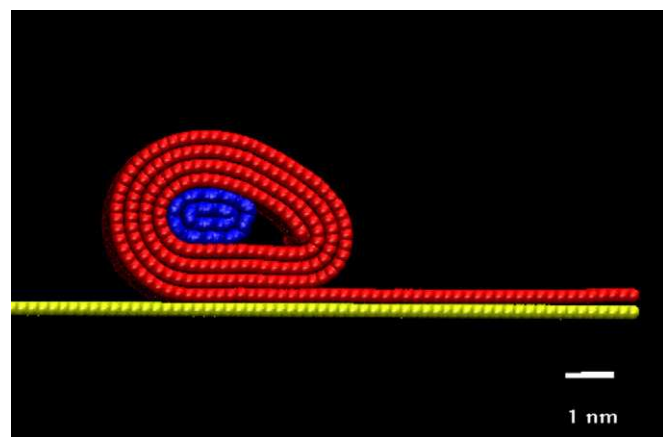
shallower well for the oscillator with a 3-walled CNT insertion. The VDW energy shows a minimum at $V = -47{,}000$ kJ/mol. The damping coefficient for this system is $\varsigma \approx 0.013$, slightly lower than for the system with a DWCNT insertion. Therefore, alternating the size of the insertion also influences the oscillatory behavior of the CNS.

3.4. Temperature effect

The effect of temperature was studied by conducting simulations at different temperatures, and the CNS position with respect to the simulation time at representative temperatures is shown in Fig. 8. The damping coefficient is $\varsigma = 0.016$ at $T = 10$ K, and $\varsigma = 0.029$ at $T = 300$ K. At higher temperatures, the damping coefficient becomes higher. The increase of damping with temperature was also observed in our earlier work on the breathing oscillation of CNS [15]. If the temperature was increased beyond 400 K, the CNS no longer showed an oscillatory behavior (interesting applications are also envisioned for CNS working at the critical damping); instead, it escaped from the local potential well and folded up rightward. Therefore, at very high temperatures, it
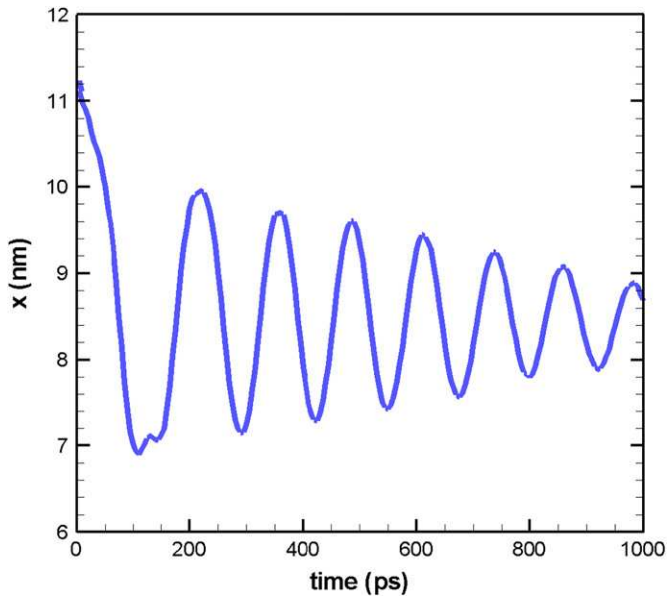
Fig. 7. The position of the CNS as a function of the simulation time for a CNS with a 3-walled MWCNT insert.
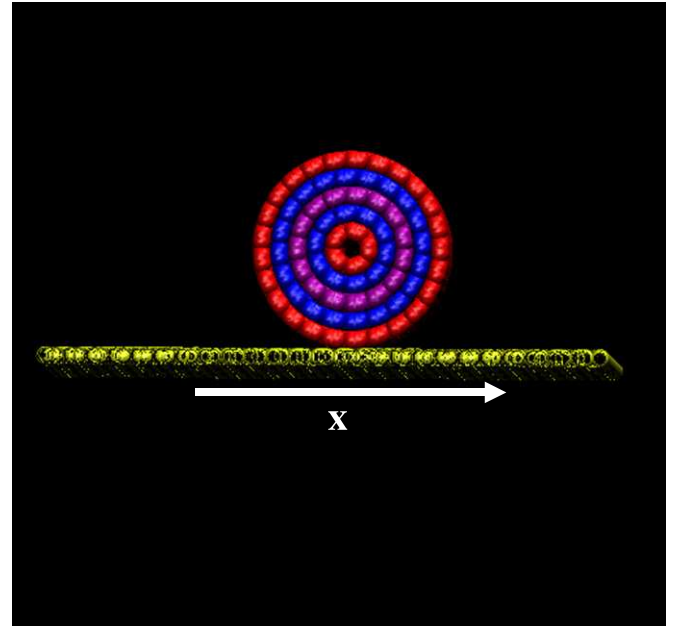

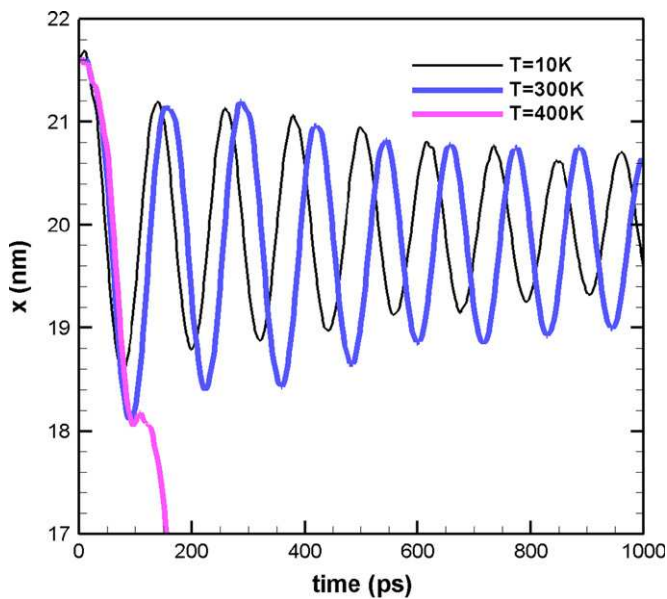Fig. 8. The position of the CNS as a function of the simulation time at representative temperatures.
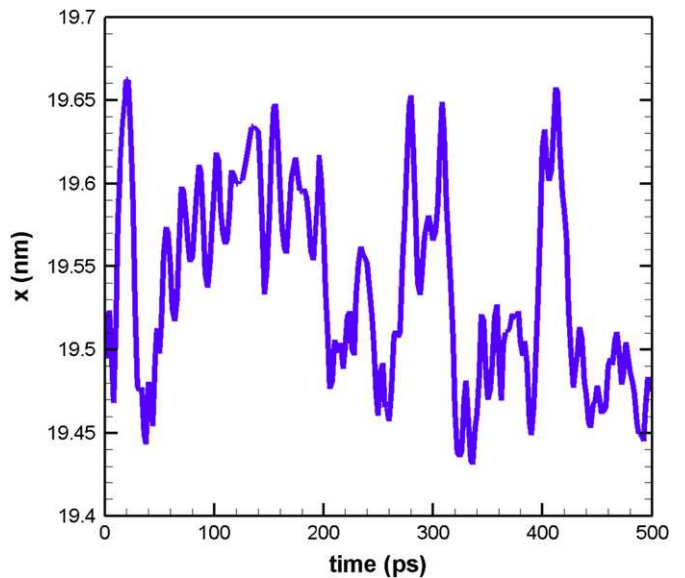

Fig. 9. Snapshots of the MWCNT on the substrate.

Fig. 10. Center of mass (COM) position of CNT in the x-direction as a function of the simulation time.

is likely for the CNS to overcome the local energy well and the system will no longer be oscillating.

3.5. MWCNT-based oscillator on a graphene substrate for comparison

It has been shown that the motion of the CNS-based oscillators on substrate can be guided and controllable. For comparison, we also studied a MWCNT-based oscillator of comparable size to that of the CNS-based one. The MWCNT consisted of five SWCNTs of types (5, 5), (10, 10), (15, 15), (20, 20), (25, 25), and 3.7 nm in length.

Initially, the MWCNT was located at the center of the substrate with the dimension of 14.4×10.5 nm^2, as shown in Fig. 9. The distance between the edge of the substrate and the CNT was

larger than 2 nm in all three dimensions, which was longer than the cutoff, 1.4 nm. MD simulation was carried out for 2 ns at an initial temperature of 10 K with the graphene substrate fixed. At the initial state of the simulation, the MWCNT rotated and translocated on the substrate. The equilibrium state was reached after 500 ps; afterwards the position of the MWCNT remained at steady values. In order to initiate oscillation from the equilibrium state, an initial velocity of 0.5 nm/s was imposed on the inner (5, 5) SWNCT for 0.5 ps in the x-direction; afterwards no external force was applied. The COM position of the MWCNT in the x-direction is shown in Fig. 10. Apparently the motion of MWCNTs on the graphene substrate is not controllable. This is in great contrast to the CNS-based oscillator, whose motion on the substrate can be guided and controlled.

4. Conclusion

In summary, we have demonstrated a substrate-supported CNS oscillator through MD simulations. It has been shown that the motion of such an oscillator on substrate is guided and can be controlled, which may offer a unique advantage over other types of oscillators, for example a system with MWCNTs on substrate. The substrate-supported CNS oscillator requires a sufficiently rigid insertion to constrain its core during oscillation, and the elastic property of the insertion influences the oscillatory behavior of the CNS. A stiffer core leads to higher frequency and smaller damping coefficient. On the other hand, a larger diameter of the insertion leads to a shallower potential well and a lower oscillatory frequency. Temperature also has a great influence on the magnitude of oscillation, and at very high temperatures the CNS is driven out of the potential well and can no longer oscillate about an equilibrium position.

Acknowledgment

References

[1] H. Shioyama, T. Akita, Carbon 41 (2003) 179.
[2] L.M. Viculis, J.J. Mack, R.B. Kaner, Science 299 (2003) 1361.
[3] M.V. Savoskin, V.N. Mochalin, A.P. Yaroshenko, N.I. Lazareva, T.E. Konstantinova, I.V. Barsukov, I.G. Prokofiev, Carbon 45 (2007) 2797.
[4] X. Xie, L. Ju, X.F. Feng, Y.H. Sun, R.F. Zhou, K. Liu, S.S. Fan, Q.Q. Li, K.L. Jiang, Nano Letters 9 (2009) 2565.
[5] Y. Chen, J. Lu, Z. Gao, Journal of Physical Chemistry C 111 (2007) 1625.
[6] S.F. Braga, V.R. Coluci, S.B. Legoas, G. Giro, D.S. Galvão, R.H. Baughman, Nano Letters 4 (2004) 881.
[7] S.F. Braga, V.R. Coluci, R.H. Baughman, D.S. Galvão, Chemical Physics Letters 441 (2007) 78.
[8] V.R. Coluci, S.F. Braga, R.H. Baughman, D.S. Galvão, Physical Review B 75 (2007) 125404.
[9] G. Mpourmpakis, E. Tylianakis, G.E. Froudakis, Nano Letters 7 (2007) 1893.
[10] H. Pan, Y. Feng, J. Lin, Physical Review B 72 (2005) 085415.
[11] X.H. Shi, N.M. Pugno, H.J. Gao, Journal of Computational and Theoretical Nanoscience 7 (2010) 1.
[12] X.H. Shi, Y. Cheng, N.M. Pugno, H.J. Gao, Small 6 (2010) 739.
[13] Q.S. Zheng, Q. Jiang, Physical Review Letters 88 (2002) 045503.
[14] P. Liu, Y.W. Zhang, C. Lu, Journal of Applied Physics 97 (2005) 094313.
[15] X.H. Shi, N.M. Pugno, Y. Cheng, H.J. Gao, Applied Physics Letters 95 (2009) 163113.
[16] X.H. Shi, Y. Cheng, N.M. Pugno, H.J. Gao, Applied Physics Letters 96 (2010) 053115.
[17] B. Hess, C. Kutzner, D. van der Spoel, E. Lindahl, Journal of Chemical Theory and Computation 4 (2008) 435.
[18] S. Andreev, D. Reichman, G. Hummer, Journal of Chemical Physics 123 (2005) 194502.
[19] M.M. Fogler, A.H. Castro Neto, F. Guinea, Physical Review B 81 (2010) 161408(R) [4 pages].